applied sciences

MDPI

Article

Development and Validation of Concept of Innovative Method of Computer-Aided Monitoring and Diagnostics of Machine Components

Krzysztof Herbuś [1,*], Andrzej Dymarek [1], Piotr Ociepka [1], Tomasz Dzitkowski [1], Cezary Grabowik [1], Kamil Szewerda [2], Katarzyna Białas [1] and Zbigniew Monica [1]

[1] Department of Engineering Processes Automation and Integrated Manufacturing Systems, Silesian University of Technology, 44-100 Gliwice, Poland; andrzej.dymarek@polsl.pl (A.D.); piotr.ociepka@polsl.pl (P.O.); tomasz.dzitkowski@polsl.pl (T.D.); cezary.grabowik@polsl.pl (C.G.); katarzyna.bialas@polsl.pl (K.B.); zbigniew.monica@polsl.pl (Z.M.)

[2] KOMAG Institute of Mining Technology, 44-101 Gliwice, Poland; kszewerda@komag.eu

* Correspondence: krzysztof.herbus@polsl.pl

Abstract: The monitoring and diagnostic system has been suggested as a non-destructive diagnostic method. The structure and operation of the suggested system can be described by the concept of digital shadow (DS). One of the main DS subsystems is a set of sensors properly placed on the monitored object and coupled with a discrete data processing model created in Matlab/Simulink. The discrete model, as another important DS subsystem of the monitored facility, transfers information about its technical condition to the operator based on data recorded by the sensor system. The digital monitoring model processes the recorded data in the form of the object's response to actions caused by its operating conditions. This work formalized a mathematical model determining the coupling of the digital model with the sensors placed on the monitored object. The formulated method using DS, due to its sensitivity, enables the detection of the damage in the object at an early stage. The tests allowed for detecting the regularities enabling the determination of the area of damage to the shaft and its size.

Keywords: monitoring and diagnostic system; digital shadow; mathematical model; synthesis of vibration systems

check for updates

Citation: Herbuś, K.; Dymarek, A.; Ociepka, P.; Dzitkowski, T.; Grabowik, C.; Szewerda, K.; Białas, K.; Monica, Z. Development and Validation of Concept of Innovative Method of Computer-Aided Monitoring and Diagnostics of Machine Components. *Appl. Sci.* **2024**, *14*, 10056. https://doi.org/10.3390/app142110056

Academic Editors: Alessandro Lo Schiavo and Xiaofeng Liu

Received: 11 September 2024
Revised: 21 October 2024
Accepted: 26 October 2024
Published: 4 November 2024

Copyright: © 2024 by the authors. Licensee MDPI, Basel, Switzerland. This article is an open access article distributed under the terms and conditions of the Creative Commons Attribution (CC BY) license (https://creativecommons.org/licenses/by/4.0/).

1. Introduction

The fourth industrial revolution, "Industry 4.0" (I4.0), determines the need to create new concepts and methods to design, manufacture and operate state-of-the-art industrial machines [1,2]. They require higher efficiency, lower operating costs, longer service life and the possibility of coupling with IT systems during the manufacturing process. With the development of IT methods, such as the Internet of Things (IOT), Artificial Intelligence (AI), and Cloud Computing (CC), machines created using these techniques began to meet new functionalities and requirements placed on them in the context of the I4.0 concept. Development of automated and flexible manufacturing systems implemented in accordance with the I4.0 concept forces manufacturers to use state-ot-the-art devices and IT technology to assess and optimize the condition of machines and the processes realized by them. Already at the design stage, virtual prototyping technology is used to enable the installation of virtual sensors and analysis of loads, vibrations and cooperation of each component before the prototype is manufactured. Numerical simulations of this type are also used during the modernization process of the existing machines, e.g., by optimizing loads [3] or identifying critical places particularly vulnerable to failure [4]. An additional aspect may be the use of co-simulation technology, thanks to which it is possible to test the correct operation of the control system or cooperation with other machines using the virtual prototype [5–8].

Intelligent sensors, state-of-the-art measuring equipment, the IOT concept, digital modelling technology and cloud data processing have allowed the development of new methods of creating the virtual equivalents of real machine components, namely, the concepts of "digital twin" (DT) and "digital shadow" (DS). Based on the literature review, from [9–16], it can be concluded that DT is a virtual representation of a real object (entity), created to optimize the processes related to it. DT is a virtual model of a product, process or service ensuring a two-way flow of information between the virtual and physical models. It enables analyzing the data and monitoring systems to avoid problems before they occur. In the case of the DT system concept, the integration of four basic elements, i.e., a graphical representation of the object, a mathematical model of the object (representing important behavior or states of the considered object or process), state monitoring system or process data, and a two-way flow of information between the virtual model and the real object, is required. The integration of these four elements makes DT an IT tool that allows for comprehensive control and optimization of the functioning of devices or processes. The DS concept, unlike the DT concept, does not have automatic feedback between the virtual model and the real object. In the DS model concept, data from a real object allow for mapping its operation and related processes, while the impact on the real object is manual. Areas of industry in which the concepts of DT and DS are used are the processes of monitoring and diagnosing the state of the machines and the processes they perform. Correct assessment of the machine state is the basis for eliminating the failures, which are one of the main causes of disruptions in manufacturing processes. They cause downtime, which negatively affects production. The use of predictive control methods, which enable predicting the current and future state of a machine or process, is important. Minimizing the costs associated with planning inspections and servicing the machines is another important aspect [17–19]. In the process of machine state control, a distinction can be made between monitoring and diagnostics. Monitoring involves measuring and recording the selected output values over time, using measuring sensors, continuously or periodically. We refer specifically to the diagnostic process when the quality criteria of the measured quantity are defined. Diagnostic assessment consists of comparing the measured value with the criterion value [20]. Diagnostic processes refer to state diagnostics and process diagnostics. State diagnostics is considered in the context of a machine's efficiency (wear or damage to its parts and assemblies), while process diagnostics is related to disruptions in the process. Of course, a machine failure directly affects the processes it realizes. Diagnosing the technical condition of a machine, according to the literature, consists of measuring methods and technologies in relation to various monitored quantities and tested physical phenomena, such as vibration diagnostics [21–26], thermal imaging diagnostics [27–34], oil diagnostics [35–40], vision diagnostics [41–43], acoustic diagnostics [44–48], or electrical diagnostics [49–62]. In relation to machines with rotating components, vibration methods are most often used. In ref. [63], it was found that state monitoring based on vibrations allows detecting of as much as 90% of faults or failures in this type of machines. Depending on the type of machines and the processes they perform, three basic diagnostic strategies are used: a single-limit strategy, which assumes that exceeding the criterion limit results in stopping the machine; a two-boundary strategy, which assumes setting two thresholds, i.e., an alarm threshold and a threshold resulting in stopping the machine; a third strategy that involves comparing the waveforms of the monitored quantity with the reference waveform [20]. In the context of the efficient functioning of the manufacturing system in accordance with the I4.0 concept, non-destructive methods of monitoring and predictive diagnosis of machines are being sought. It is particularly important that these methods are sensitive and enable the detection of small changes in the monitored object at an early stage of damage propagation. This is important for planning the necessary machine downtime in advance.

Currently, one of the most dynamically developing methods of monitoring and non-destructive diagnostics is vibration methods. This is mainly due to the emergence of small wireless sensors based on IoT technology, which makes continuous monitoring of

the machine possible. This allows one to improve, and in advanced applications fully automate, the diagnostic reasoning process. This is important in the context of the I4.0 approach. Then, expensive, specialized and often invasive ad hoc inspection of machines is not required, but only automatic or remote analysis of continuously recorded data is needed. Therefore, structural health monitoring (SHM) methods based on the analysis of dynamic parameters of systems are currently being dynamically developed by researchers from many academic centers [64–69].

The development of these methods results from the need to optimize costs related to broadly understood machine maintenance. Some of these methods make it possible not only to detect damage at the initial stage of its occurrence but also to localize it in the machine structure. These methods must then be highly sensitive to changes in the analyzed parameters. One of the most important groups in this context is model-based vibration methods. Vibration diagnostics based on a dynamic model consists of comparing the dynamic parameters identified for an undamaged object with the parameters measured during its operation. Based on the identified differences, it is possible to detect damage and the place of its occurrence [70–72].

In general, such methods can be divided based on the assessment of changes in the natural frequency, damping coefficient, natural vibration modes or frequency characteristics. In the case of methods based on the assessment of the change in the natural frequency or the change in the damping coefficient, they are characterized by low sensitivity to small damages, and it is difficult to locate the place where the damage occurred [73–79]. However, methods that analyze changes in frequency characteristics, filtered with respect to the selected natural frequency, do not provide information on the location of the detected damage. In the case of methods based on the assessment of natural vibration modes (modal methods), it is necessary to use a sufficiently large number of measurement points, which significantly increases the costs of using these methods. Often, due to the insufficient number of measurement points, the use of these methods is burdened with a large error and difficulty in locating the place of damage occurrence.

An important aspect of assessing the condition of an object is the ability to identify and predict damage propagation. Evaluating the rate of propagation and the probability of catastrophic failure forms the basis for determining the feasibility and duration of safe operation. This enables controlled decisions regarding the timing of repairs or the moment when the object must be decommissioned. In this context, methods and algorithms are used to predict the rate and nature (direction) of damage propagation, allowing for an assessment of the object's future condition. These methods include those based on artificial intelligence (Neural Networks, Artificial Immune Systems (AIS)) [80–84], algorithms based on the domino effect [85,86], experience-based methods (Case-Based Reasoning (CBR)) [87,88], and numerical methods that enable computer simulations of damage propagation (FEM, BEM) [89]. Accurate assessment of damage propagation allows for predicting the future condition of the object, which enhances safety and reduces the costs associated with its operation.

The presented research work describes the concept of a monitoring and diagnostic system based on the vibration diagnostics method with the structure of the DS system. The proposed system is a set of sensors placed on the monitored machine component and coupled with a discrete data processing model created in the Matlab/Simulink program. The discrete model serves as a digital monitoring system that, based on recorded data, transmits information about the technical state of the monitored machine component to the user. The digital monitoring system processes the acquired data in the form of the object's response to the action caused by its operating conditions. The time processes obtained in this way (system responses) are processed by a digital monitoring model and compared with the previously generated waveforms of the tested machine component. The data generated by the system (compared to the pattern) indicate the area and amount of damage in the tested object. Monitoring is continuous throughout the entire time of the facility operation, with simultaneous processing of recorded data in the DS [90–92]. Detection of

ongoing changes is possible thanks to the use of a mathematical model, which determines its appropriate coupling with sensors placed on the monitored machine component. This research work formulates and formalizes the mathematical model on the basis of which the DS was built. Correct operation of the DS was verified using the model of a continuous (real) system in the form of a multi-stage machine shaft, modelled in the PLM Siemens NX program. Sensors were placed on the shaft in selected places to record data during the simulation of shaft operation. In the next stage, the data were sent to a digital monitoring system to compare them with the previously generated pattern. During the tests, various types of damage were introduced into the monitored facility, and the data were recorded and processed in DS. The data were compared with the pattern, which allowed us to detect the location and extent of damage to the monitored object.

2. Description of the Tested Machine Component

This paper discusses the problem of monitoring and diagnostics of the gear shaft. It is assumed that the proposed methodology will enable monitoring and diagnosis of its technical state. The real object was replaced by a 3D model and the simulation results of the model's operation were considered equivalent to the results from the operation of the real system in relation to the considered problem. The developed 3D model of the system in the form of a model prepared for motion simulation consists of a six-stage shaft with bearings, a gear wheel and a half clutch (Figure 1). To recreate the operation of a real machine component in its working environment, the Motion module of the PLM Siemens NX 2306 software was used. In the proposed model, the operating mode of one of the bearings was modelled in the form of a rotational constraint corresponding to a class V kinematic pair (fixed support—only rotation around the shaft axis is possible), while the other bearing was modelled in the form of a cylindrical constraint corresponding to a class IV kinematic pair (movable support—rotation around the shaft axis and axial displacement are possible).

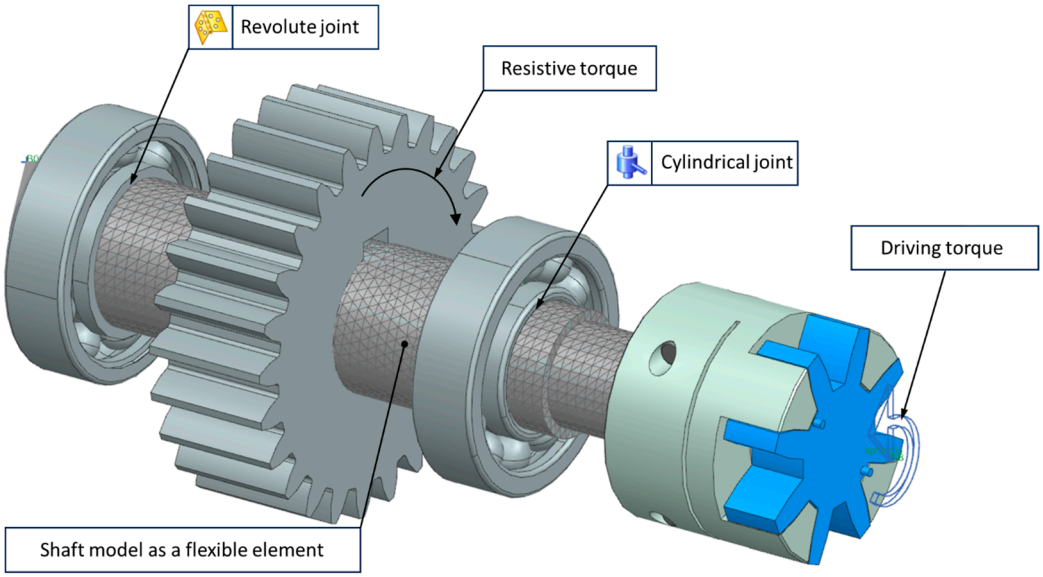


Figure 1. Tested object in the form of a 3D model of a shaft in the context of its operating conditions.

The force that sets the modelled system into motion is transmitted through the coupling connection with the shaft end journal. It was assumed, in accordance with the operating conditions of the real system, that the driving torque applied to the end shaft journal causes its movement at a rotational speed of 3000 rpm, assuming that a resistive torque of 100 Nm acts on the gear wheel.

Due to the fact that the considered problem is related to monitoring the technical condition of the shaft, it was modelled as a flexible body. The flexible component was

mounted in accordance with the previously described method, and additionally, a gear wheel and half of the clutch were mounted on the deformable shaft model. It should be emphasized that all components of the assembly affect the deformable shaft model through defined constraints using one-dimensional (1D) finite elements spanned on the separated surfaces of the shaft model. It was assumed that testing such a separated gear component would be representative in relation to the considered problem.

3. Digital Monitoring System

This section describes the components of a digital monitoring system whose task is to detect damage to the monitored machine component. The proposed digital monitoring system, which is coupled to the tested object, is composed of discrete inertial and elastic components (Figure 2). The number of degrees of freedom of the system (inertial elements) corresponds to the number of sensors (accelerometers) directly related to the monitored real machine component. The parameters of the digital monitoring system (parameters of elastic components) are estimated on the basis of the adopted mass distribution (RFE method) and the determined natural frequencies of the real object, which were obtained through comparative synthesis.

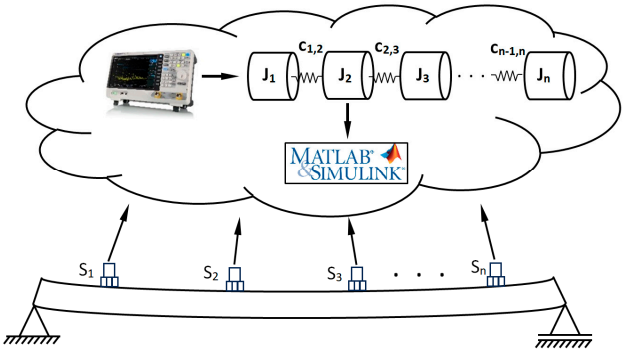


Figure 2. The concept of a digital monitoring system coupled with the monitored object.

3.1. Mathematical Model of a Digital Monitoring System

Data from monitoring of real machine components during their operation are verified and then processed by a digital monitoring system. As a result of passing the data through the digital system, response characteristics of the system are obtained, on the basis of which it is possible to observe and locate damage to the monitored object, evidenced by the deviation of the response characteristics of the damaged system from the characteristics of the reference system [93]. Observation of the deviation of the characteristics is possible by using the suggested mathematical model. The suggested method is a non-destructive vibration method, but unlike the classic methods used in diagnostics, it allows the location of damage with high precision at its low values, while the comparison of frequency/amplitude characteristics does not provide satisfactory results. In the next stage of this work, the mathematical model of the digital monitoring system was formalized on the example of a system simulating the reading of data from two sensors (accelerometers).

The obtained responses of the monitored system for a system with two degrees of freedom, assuming a failure in the system, are the sum of the general and specific solutions of the differential equations of the object whose natural frequencies are equal to $\omega_0 = 0$, $\omega_{12}^2 = \omega_1^2 + \omega_2^2 = \frac{(c-\Delta c)}{m_1} + \frac{(c-\Delta c)}{m_2}$. The mathematical model for the digital monitoring system takes the form of a system of differential motion equations presented in Equation (1).

$$\begin{cases} m_1\ddot{x}_{11} + c(x_1 - x_2) = F_0 \sin\omega t \\ m_2\ddot{x}_{22} + c(x_2 - x_1) = 0 \end{cases} \quad (1)$$

where x_1, x_2 represent the data read out from the sensors monitoring the object, and x_{11}, x_{22} represent the response of the digital monitoring system.

Applying the Laplace transform in Equation (1) and taking into account Equation (2), the following form is obtained:

$$\begin{cases} m_1 s^2 X_{11}(s) + c\left(A\frac{1}{s^2} - B\frac{\omega_{12}}{(s^2+\omega_{12}^2)} + C\frac{\omega}{(s^2+\omega^2)}\right) - c\left(A\frac{1}{s^2} - D\frac{\omega_{12}}{(s^2+\omega_{12}^2)} + E\frac{\omega}{(s^2+\omega^2)}\right) = \frac{F_0\omega}{s^2+\omega^2} \\ m_2 s^2 X_{22}(s) + c\left(A\frac{1}{s^2} - D\frac{\omega_{12}}{(s^2+\omega_{12}^2)} + E\frac{\omega}{(s^2+\omega^2)}\right) - c\left(A\frac{1}{s^2} - B\frac{\omega_{12}}{(s^2+\omega_{12}^2)} + C\frac{\omega}{(s^2+\omega^2)}\right) = 0 \end{cases} \quad (2)$$

where $A = \frac{\beta\omega_2^2}{\omega\omega_{12}^2}$, $B = \frac{\beta\omega(\omega_2^2-\omega_{12}^2)}{\omega_{12}^3(\omega_{12}^2-\omega^2)}$, $C = \frac{\beta\omega(\omega^2-\omega_2^2)}{\omega^2(\omega_{12}^2-\omega^2)}$, $D = \frac{\beta\omega\omega_2^2}{\omega_{12}^3(\omega_{12}^2-\omega^2)}$, $E = \frac{\beta\omega_2^2}{\omega^2(\omega_{12}^2-\omega^2)}$

$$\begin{cases} X_{11}(s) = \frac{\beta\omega}{s^2(s^2+\omega^2)} - \frac{\omega_{10}^2}{s^2}\left(\frac{\beta\omega(s^2+\omega_2^2)}{s^2(s^2+\omega_{12}^2)(s^2+\omega^2)} - \frac{\omega_2^2\beta\omega}{s^2(s^2+\omega_{12}^2)(s^2+\omega^2)}\right) \\ X_{22}(s) = \frac{\omega_{20}^2}{s^2}\left(\frac{\beta\omega(s^2+\omega_2^2)}{s^2(s^2+\omega_{12}^2)(s^2+\omega^2)} - \frac{\omega_2^2\beta\omega}{s^2(s^2+\omega_{12}^2)(s^2+\omega^2)}\right) \end{cases} \quad (3)$$

where $\omega_{10}^2 = \frac{c}{m_1}$, $\omega_{20}^2 = \frac{c}{m_2}$, $\beta = \frac{F_0}{m_1}$.

As a result of the transformations, the system of equations takes the following form:

$$\begin{cases} X_{11}(s) = \frac{\beta\omega(s^2+\omega_2^2-\Delta\omega_1^2)}{s^2(s^2+\omega^2)(s^2+\omega_{12}^2)} \\ X_{22}(s) = \frac{\omega_{20}^2\beta\omega}{s^2(s^2+\omega_{12}^2)(s^2+\omega^2)} \end{cases} \quad (4)$$

After decomposing the functions of the system of Equation (4) into simple fractions, the responses of the digital monitoring system are obtained in the form of a function of the Laplace variable for the case of the tested object with damage.

$$X_{11}(s) = \frac{\beta(\omega_2^2-\Delta\omega_1^2)}{\omega\omega_{12}^2}\frac{1}{s^2} - \frac{\beta\omega(\omega_2^2-\Delta\omega_1^2-\omega_{12}^2)}{\omega_{12}^3(\omega_{12}^2-\omega^2)}\frac{\omega_{12}}{(s^2+\omega_{12}^2)} + \frac{\beta\omega(\omega^2-\omega_2^2+\Delta\omega_1^2)}{\omega^2(\omega_{12}^2-\omega^2)}\frac{\omega}{(s^2+\omega^2)} \quad (5)$$

$$X_{22}(s) = \frac{\beta\omega_{20}^2}{\omega\omega_{12}^2}\frac{1}{s^2} - \frac{\beta\omega\omega_{20}^2}{\omega_{12}^3(\omega_{12}^2-\omega^2)}\frac{\omega_{12}}{(s^2+\omega_{12}^2)} + \frac{\beta\omega_{20}^2}{\omega^2(\omega_{12}^2-\omega^2)}\frac{\omega}{(s^2+\omega^2)} \quad (6)$$

Using the inverse Laplace transform, Equations (5) and (6) take the final form of the response of the digital monitoring system as a function of the time variable:

$$x_{11}(t) = \frac{\beta(\omega_2^2-\Delta\omega_1^2)}{\omega\omega_{12}^2}t - \frac{\beta\omega(\omega_2^2-\Delta\omega_1^2-\omega_{12}^2)}{\omega_{12}^3(\omega_{12}^2-\omega^2)}\sin\omega_{12}t + \frac{\beta\omega(\omega^2-\omega_2^2+\Delta\omega_1^2)}{\omega^2(\omega_{12}^2-\omega^2)}\sin\omega t \quad (7)$$

$$x_{22}(st) = \frac{\beta\omega_{20}^2}{\omega\omega_{12}^2}t - \frac{\beta\omega\omega_{20}^2}{\omega_{12}^3(\omega_{12}^2-\omega^2)}\sin\omega_{12}t + \frac{\beta\omega_{20}^2}{\omega^2(\omega_{12}^2-\omega^2)}\sin\omega t \quad (8)$$

Similarly, the case of a digital monitoring system for an object without damage was considered, assuming that x_1 and x_2 are the solutions of such a system. The obtained responses of the Laplace function then take the following form:

$$X_{10}(s) = \frac{\beta\omega_{20}^2}{\omega\omega_{120}^2}\frac{1}{s^2} - \frac{\beta\omega(\omega_{20}^2-\omega_{120}^2)}{\omega_{120}^3(\omega_{120}^2-\omega^2)}\frac{\omega_{120}}{(s^2+\omega_{120}^2)} + \frac{\beta\omega(\omega^2-\omega_{20}^2)}{\omega^2(\omega_{120}^2-\omega^2)}\frac{\omega}{(s^2+\omega^2)} \quad (9)$$

$$X_{20}(s) = \frac{\beta\omega_{20}^2}{\omega\omega_{120}^2}\frac{1}{s^2} - \frac{\beta\omega\omega_{20}^2}{\omega_{120}^3(\omega_{120}^2-\omega^2)}\frac{\omega_{12}}{(s^2+\omega_{120}^2)} + \frac{\beta\omega_{20}^2}{\omega^2(\omega_{120}^2-\omega^2)}\frac{\omega}{(s^2+\omega^2)} \quad (10)$$

where $\omega_{120}^2 = \omega_{10}^2 + \omega_{20}^2 = \frac{c}{m_1} + \frac{c}{m_2}$.

As a result of the application of the inverse Laplace transform, the response of the digital monitoring system for an object without damage as a function of the time variable takes the following form:

$$x_{10}(t) = \frac{\beta\omega_{20}^2}{\omega\omega_{120}^2}t - \frac{\beta\omega\left(\omega_{20}^2 - \omega_{120}^2\right)}{\omega_{120}^3\left(\omega_{120}^2 - \omega^2\right)}\sin\omega_{12}t + \frac{\beta\omega\left(\omega^2 - \omega_{20}^2\right)}{\omega^2\left(\omega_{120}^2 - \omega^2\right)}\sin\omega t \tag{11}$$

$$x_{20}(t) = \frac{\beta\omega_{20}^2}{\omega\omega_{120}^2}t - \frac{\beta\omega\omega_{20}^2}{\omega_{120}^3\left(\omega_{120}^2 - \omega^2\right)}\sin\omega_{12}t + \frac{\beta\omega_{20}^2}{\omega^2\left(\omega_{120}^2 - \omega^2\right)}\sin\omega t \tag{12}$$

In the case of the determined quantities (x_{10}, x_{11}, x_{20}, x_{22}), their components of the obtained sum were compared, in particular the slope coefficient of the linear t function. The determined slope coefficients assume the value for the following cases:

- without damage,

$$x_{10} = x_{20} = \frac{\beta\omega_{20}^2}{\omega\omega_{120}^2} \tag{13}$$

- with damage,

$$x_{11} = \frac{\beta\left(\omega_2^2 - \Delta\omega_1^2\right)}{\omega\omega_{12}^2},\ x_{22} = \frac{\beta\omega_{20}^2}{\omega\omega_{12}^2} \tag{14}$$

Based on the comparison of the values described in (13) and (14), the following inequality can be observed:

$$\omega_{20}^2 > \left(\omega_2^2 - \Delta\omega_1^2\right) \tag{15}$$

$$\omega_{120}^2 > \omega_{12}^2 \tag{16}$$

As a result of the above, it is concluded that the linear functions of the determined responses (x_{10}, x_{11}, x_{20}, x_{22}) are different, which is presented in functions (17) and (18).

$$\frac{\beta\omega_{20}^2}{\omega\omega_{120}^2} = \frac{\beta\omega_2^2}{\omega\omega_{12}^2} > \frac{\beta\left(\omega_2^2 - \Delta\omega_1^2\right)}{\omega\omega_{12}^2} \tag{17}$$

$$\frac{\beta\omega_{20}^2}{\omega\omega_{120}^2} = \frac{\beta\omega_2^2}{\omega\omega_{12}^2} < \frac{\beta\omega_{20}^2}{\omega\omega_{12}^2} \tag{18}$$

A comparison of the slope coefficients of the linear function of the response sum component before (x_{10}, x_{20}) and after damage (x_{11}, x_{22}) indicates their different values, which consequently leads to the deviation of the linear functions relative to each other. In the case of the discussed example, the characteristics converge, indicating the location of the damage, and the tangent of the inclination angle in relation to the pattern indicates its size. It should be noted that the deviation of the characteristics from the pattern depends on the place of the applied force. In the discussed case, the deviation of the characteristics from the point of damage would occur assuming a force imposed on the mass m_2. Based on the comparison of response solutions before and after damage, without taking into account the suggested mathematical model, the solutions do not show a change in the tangent of the slope angle of the angular coefficients, always maintaining the same value.

3.2. Structure and Parameters of the Digital Monitoring System

This section presents issues related to determining the structure and parameters of the digital monitoring system used in the diagnostic device of the analyzed real machine component. The operating driving shaft is the real object, the analysis of which requires monitoring its rotational motion. Therefore, the physical model of a digital monitoring system is a discrete torsional vibrating system. Such a model consists of non-deformable discs with one degree of freedom and elastic components constituting connections between

weightless shaft sections, transmitting only torques. The structure of the digital monitoring system is implied by the analyzed real system and the number of installed sensors monitoring it. Within the analyzed shaft, three critical areas were identified that should be monitored and diagnosed (Figure 3a), which correspond to the number of areas between the components cooperating with the shaft: bearings, gear wheel and clutch. On this basis, the arrangement of four sensors (S1, S2, S3 and S4) detecting angular displacement at the ends of these areas was assumed (Figure 3b).

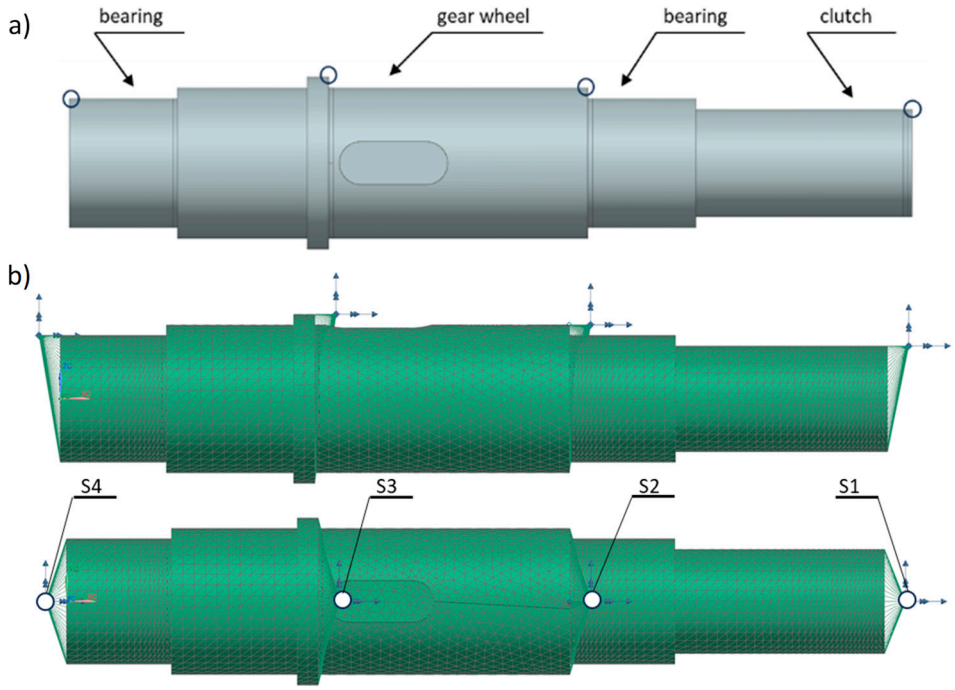


Figure 3. Separated monitoring and diagnostic areas with the arrangement of sensors. (**a**) Critical areas of the analyzed shaft; (**b**) The arrangement of sensors detecting angular displacement at the ends of critical areas.

In the analyzed case, the test was carried out on the driving shaft on which four measuring points were installed. Therefore, a single-axis discrete physical model with four degrees of freedom is the structure of the digital monitoring system (Figure 4).

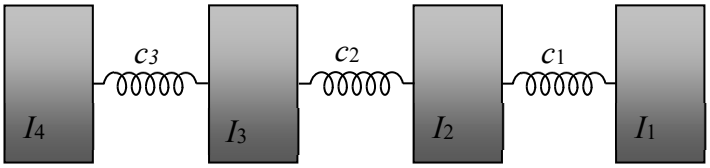


Figure 4. Structure of a discrete physical model with four degrees of freedom.

The adopted physical model is a free system (the inertial components are not connected to the support via springs), indicating the possibility of rotational motion as one rigid body. This causes the frequency of first natural vibrations to be zero. For the system structure adopted in this way, its dynamic parameters should be determined to meet specific dynamic properties, in the form of the first four frequencies of torsional vibrations of the analyzed object (taking into account the first zero value). For the purposes of estimating the parameters of the discrete model, the forms and values of the natural vibrations frequencies of the analyzed component were determined (Figure 5). The Pre/Post module based on the finite element method of the PLM Siemens NX 2306 software was used to determine the form and value of the shaft's own vibration frequency. The following basic parameters

were adopted in the analysis in relation to the finite element mesh: type of finite element—CTETRA (10—ten nodes), size of finite element—2.65 mm.

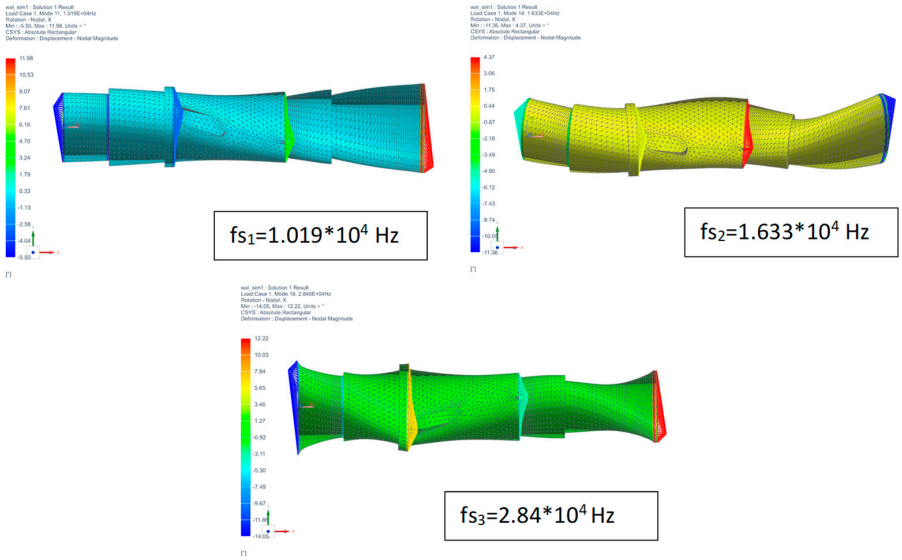


Figure 5. Graphical representation of the first three forms of torsional vibrations of the analyzed shaft along with their values.

Limiting the input data only to natural frequencies makes it impossible to use the synthesis apparatus [94,95] directly to determine the required dynamic parameters. At the same time, the use of the method of discretization of a continuous system, in relation to the adopted number of degrees of freedom, is subject to high calculation inaccuracy (due to the natural frequencies of the analyzed object). For this purpose, a combined method was suggested to determine the dynamic parameters of a discrete physical model. In the first step, the mass moments of inertia of non-deformable discs with one degree of freedom are determined. The rigid finite element method (RFEM) is used for this purpose, on the basis of which the system is divided into RFEMs (Figure 6), and on this basis, the mass moments of inertia relative to the main central axes of inertia of each RFEM are determined.

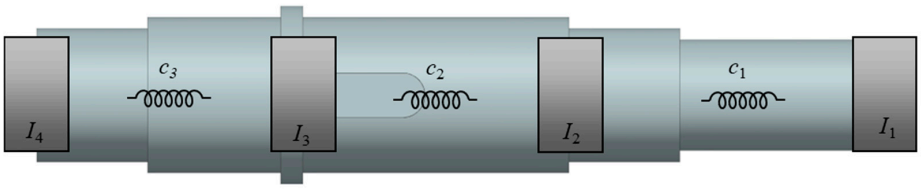


Figure 6. Scheme of dividing the drive shaft into RFE.

Each mass moment of inertia of non-deformable discs with one degree of freedom, for such a division of the system (Figure 6), is as follows: $I_1 = 11.26 \cdot 10^{-6}$ kgm^2, $I_2 = 53.93 \cdot 10^{-6}$ kgm^2, $I_3 = 71.31 \cdot 10^{-6}$ kgm^2, $I_4 = 21.34 \cdot 10^{-6}$ kgm^2.

In the next step, after determining the inertial parameters of the model, the elastic parameters of the discrete physical model should be determined. It should be borne in mind that each physical parameter has a significant impact on the distribution of the resonant and anti-resonant zones of the vibrating system. In order to meet the requirements in terms of dynamic properties, in the form of the first four frequencies of torsional vibrations of the analyzed object (taking into account the first zero value), the comparative synthesis method was used to determine the searched parameters [94–96]. For this purpose, based on the adopted structure of the discrete model of a physical system, dynamic stiffness

matrices are built in the following form (taking into account the numerical parameters of the determined inertial parameters):

$$\mathbf{Z_s}(s) = \begin{bmatrix} I_1 s^2 + c_1 & -c_1 & 0 & 0 \\ -c_1 & I_2 s^2 + c_1 + c_2 & -c_2 & 0 \\ 0 & -c_2 & I_3 s^2 + c_2 + c_3 & -c_3 \\ 0 & 0 & -c_3 & I_4 s^2 + c_3 \end{bmatrix} \quad (19)$$

where, based on the stiffness matrix Z(s), the following polynomial is determined:

$$\det(\mathbf{Z_s}(s)) = A_8 s^8 + A_6 s^6 + A_4 s^4 + A_2 s^2 \quad (20)$$

where $A_8 = 9.23889 \cdot 10^{-19}$, $A_6 = 9.91746 \cdot 10^{-14} \cdot c_1 + 3.00881 \cdot 10^{-14} \cdot c_2 + 5.62608 \cdot 10^{-14} \cdot c_3$, $A_4 = 2.91214 \cdot 10^{-9} \cdot c_1 c_2 + 6.03929 \cdot 10^{-9} \cdot c_1 c_3 + 1.65052 \cdot 10^{-9} \cdot c_2 c_3$, $A_2 = 1.57831 \cdot 10^{-4} c_1 c_2 c_3$.

To calculate the values of elastic parameters, the obtained polynomial should be divided by the coefficient A_8 and then compared to the polynomial characterizing the adopted dynamic properties in the form of four natural frequencies of the system. This equation takes the following form:

$$\frac{\det(\mathbf{Z_s}(s))}{A_8} = s^2 \prod_{i=2}^{n} \left(s^2 + {\omega_{bi}}^2 \right) \quad (21)$$

where $\omega_{b1} = 64{,}025.7$ rad/s, $\omega_{b2} = 102{,}604$ rad/s, $\omega_{b3} = 178{,}442$ rad/s.

After comparing the coefficients with the same powers of the polynomial of Equation (21), a system of equations is built, on the basis of which the elastic parameters are determined. The dynamic parameters of the searched elastic elements, in the case of the structure shown in Figure 6, are listed in Table 1.

Table 1. Dynamic parameters of the searched elastic elements.

i	c_i [Nm/rad]					
1	44.311	47.100	89.152	113.457	281.482	290.282
2	906.273	344.402	176.354	906.689	345.517	176.508
3	200.305	495.875	511.619	78.194	83.189	156.993

All obtained sets of elastic parameter solutions meet the adopted requirements regarding the dynamic properties, in the form of the first four frequencies of torsional vibrations of the analyzed object. From this set, a solution was selected whose parameters were closest to the stiffnesses determined by the RFE method. This solution was the second set of parameters listed in the table. As a result of the calculations, a set of all dynamic parameters of a discrete physical model was obtained, constituting the structure of a digital monitoring system used to detect damage to the tested object.

4. Developed Testing Methodology and Test Results

This section describes the developed testing methodology for monitoring and diagnostics of the condition of the tested machine component with computer aid. It also describes the creation of reference characteristics and the process of monitoring the condition of the machine component using illustrations of the operation of the digital shadow and presents the test results.

4.1. Testing Methodology in the Planned Experiment

To create a digital shadow, in accordance with the terminology used in the analyzed literature, it is necessary to create a digital model of the real machine component and ensure a continuous one-way flow of information from the real object to the digital model. The research work presents an illustration of the digital shadow operation, where the real object was replaced by the created 3D model (Figure 7) and the angular displacements of each

sensor placed on the model were considered to be equivalent to the values that would occur during operation of the real system.

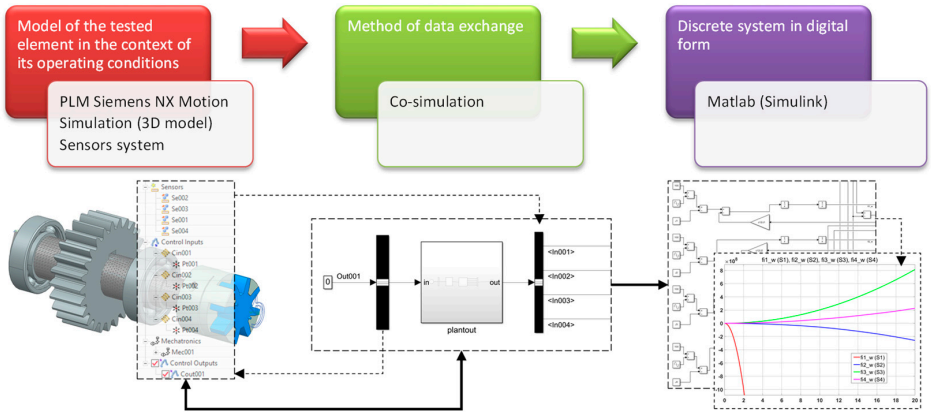


Figure 7. Graphical representation of the formulated monitoring method using DS.

For this purpose, a 3D model of the analyzed real machine component was developed in the form of a system prepared for simulation of motion using the Motion module of PLM Siemens NX 2306 software. The digital model was built in the form of a discrete vibrating system in Matlab/Simulink R2021a software. Ensuring continuous, one-way data exchange was achieved by using co-simulation between the Motion module of the PLM Siemens NX 2306 software and the Matlab/Simulink R2021a program.

The developed monitoring method using DS was first used to determine the reference characteristics. The reference characteristics (Figure 8) are created as follows:

- The angular displacements are measured and recorded in the time domain using the adopted sensor system (sensors S1, S2, S3 and S4);
- The recorded angular displacements are transferred via co-simulation to the discrete model in digital form;
- Solving the task of determining the waveform of variability of the angular displacement of the inertial elements of the discrete model allows for the determination of the reference characteristics (S1w, S2w, S3w, S4w). It was assumed that the obtained waveforms constitute the "0 line" of reference in relation to the characteristics of the monitored machine component recorded in the same way.

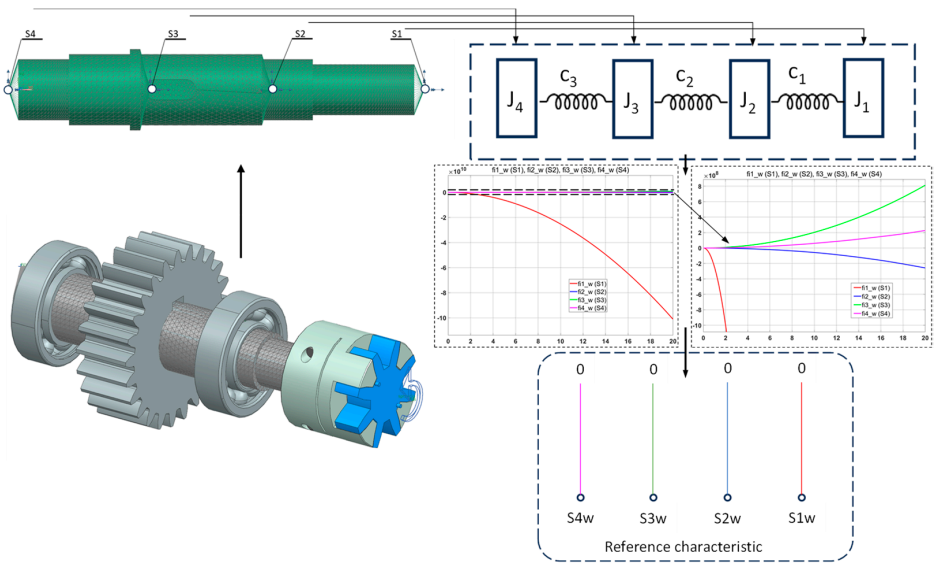


Figure 8. Determination of reference characteristics using the developed methodology.

The monitoring and diagnostics of the state of the tested machine component using the developed testing methodology consist of recording the current characteristics of the system in use (S1u, S2u, S3u, S4u) and comparing them with the previously developed reference characteristics (Figure 9).

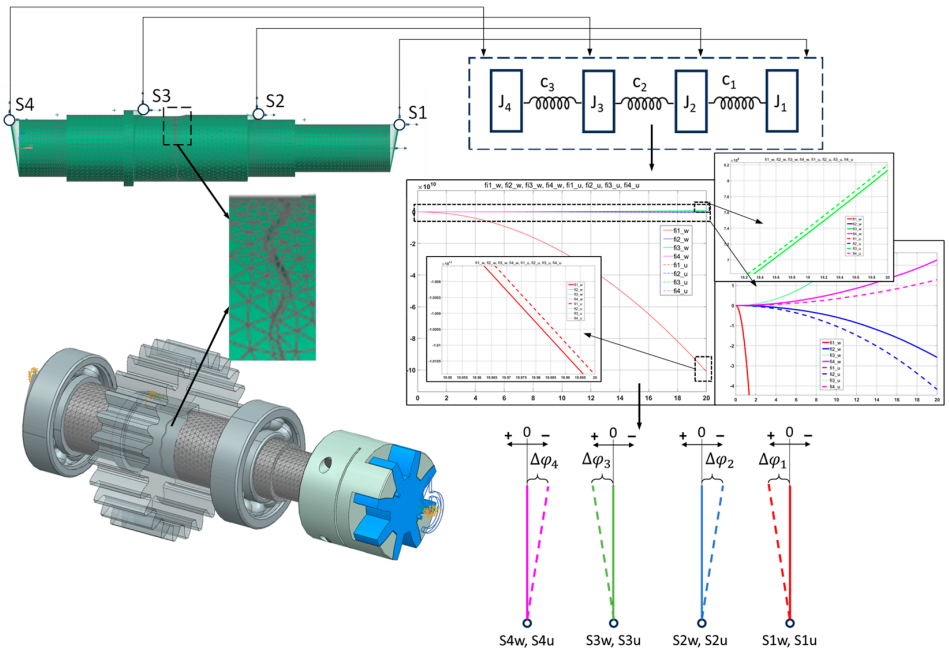


Figure 9. Monitoring and diagnostics of the tested machine component state using the developed methodology.

Based on the deviation of the current characteristic from the reference one and the value of this deviation, inference rules can be defined to identify the area of possible damage to the monitored machine component.

4.2. Test Results

As part of this research work, a series of tests were conducted to confirm the method formalized in this work with respect to its possibility of using it to identify the area of damage in the monitored machine component (Tables 2–4). The tests consisted of introducing the damage to a given shaft stage and determining the characteristics of the monitored machine component state using the developed methodology, taking into account its operating environment (Section 2).

Based on the obtained test results, it can be seen that there are deviations in the state characteristics of the tested machine component in all tested intervals, regardless of the location of its damage. However, in the case of the theoretical model (discrete systems), deviations in the characteristics occur only on the displacements of inertial elements between which a change in stiffness has been introduced. The remaining inertial elements of the theoretical model would overlap the current characteristic with the reference characteristic ($\Delta\varphi_n = 0$). Therefore, in the tested system, an additional criterion for the deviation of the current characteristics from the reference ones was adopted. The process of identifying the area where damage occurs can therefore be presented in the following steps:

- Identify in the characteristics of the machine component's state the form of deviation of the current characteristic from the reference characteristic consistent with theoretical considerations (the characteristics between two sensors defining the searched area with damage should form a minority sign when viewed from the bottom of the characteristics);

- If the state characteristics contain only one form of deviation consistent with theoretical considerations, the damaged area is located between the sensors on which these deviations were recorded (Table 2, items 4 to 7, Table 3, items 1 to 6, Table 4, item 4);
- If the state characteristics appear more than once in a form consistent with theoretical considerations, then the sum of the absolute values of deviations between the sensors monitoring these areas should be taken into account. The damaged area should have a higher value of the described sum (Table 2, items 2 to 4, Table 4, item 1).

Table 2. Determining the characteristics of the monitored machine component state when introducing damage in the area confined by sensors S1 and S2.

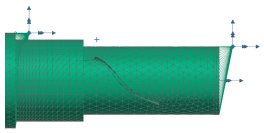
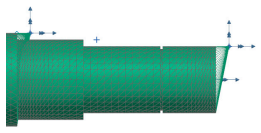
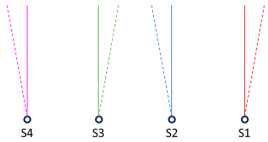
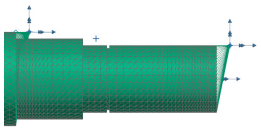
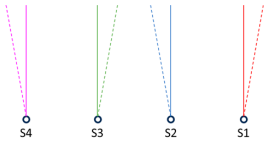
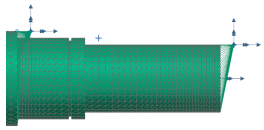
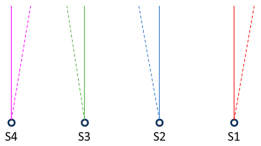
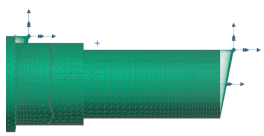
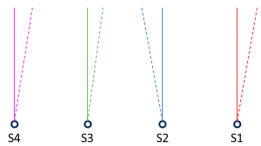
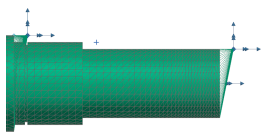
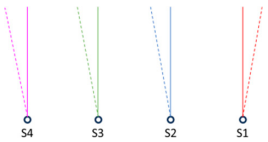
Geometric Form and Place of Damage	Characteristics of Monitored Machine Component State	Deviation of the Characteristics [rad]	Volume Loss [%]	Natural Vibrations Frequency [Hz]
No damage		$\Delta\varphi_1 = 0$ $\Delta\varphi_2 = 0$ $\Delta\varphi_3 = 0$ $\Delta\varphi_4 = 0$	0	$f_1 = 3.995 * 10^3$ $f_2 = 4.063 * 10^3$ $f_3 = 9.015 * 10^3$ $f_4 = 9.163 * 10^3$
		$\Delta\varphi_1 = -4.148 * 10^8$ $\Delta\varphi_2 = 9.628 * 10^7$ $\Delta\varphi_3 = -4.56 * 10^5$ $\Delta\varphi_4 = 7.863 * 10^6$	0.02	$f_1 = 3.995 * 10^3$ $f_2 = 4.059 * 10^3$ $f_3 = 9.012 * 10^3$ $f_4 = 9.142 * 10^3$
		$\Delta\varphi_1 = -1.536 * 10^9$ $\Delta\varphi_2 = 3.31 * 10^8$ $\Delta\varphi_3 = -1.332 * 10^6$ $\Delta\varphi_4 = 6.848 * 10^7$	0.05	$f_1 = 3.996 * 10^3$ $f_2 = 4.064 * 10^3$ $f_3 = 9.004 * 10^3$ $f_4 = 9.149 * 10^3$
		$\Delta\varphi_1 = -1.519 * 10^9$ $\Delta\varphi_2 = 3.148 * 10^8$ $\Delta\varphi_3 = -2.271 * 10^5$ $\Delta\varphi_4 = 2.232 * 10^7$	0.05	$f_1 = 3.979 * 10^3$ $f_2 = 4.047 * 10^3$ $f_3 = 8.948 * 10^3$ $f_4 = 9.104 * 10^3$
		$\Delta\varphi_1 = -5.297 * 10^8$ $\Delta\varphi_2 = 1.236 * 10^8$ $\Delta\varphi_3 = -1.161 * 10^6$ $\Delta\varphi_4 = 1.15 * 10^8$	0.06	$f_1 = 3.985 * 10^3$ $f_2 = 4.052 * 10^3$ $f_3 = 9.000 * 10^3$ $f_4 = 9.146 * 10^3$
		$\Delta\varphi_1 = -4.69 * 10^8$ $\Delta\varphi_2 = 1.718 * 10^8$ $\Delta\varphi_3 = -1.497 * 10^6$ $\Delta\varphi_4 = -8.085 * 10^7$	0.03	$f_1 = 3.980 * 10^3$ $f_2 = 4.046 * 10^3$ $f_3 = 8.993 * 10^3$ $f_4 = 9.140 * 10^3$
		$\Delta\varphi_1 = -7.469 * 10^8$ $\Delta\varphi_2 = 1.95 * 10^8$ $\Delta\varphi_3 = 1.71 * 10^6$ $\Delta\varphi_4 = 2.229 * 10^7$	0.06	$f_1 = 3.968 * 10^3$ $f_2 = 4.033 * 10^3$ $f_3 = 8.998 * 10^3$ $f_4 = 9.145 * 10^3$

Table 3. Determining the characteristics of the monitored machine component state when introducing damage in the area confined by sensors S2 and S3.

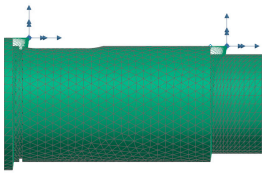
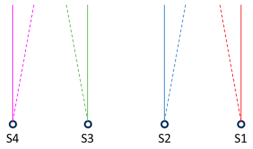
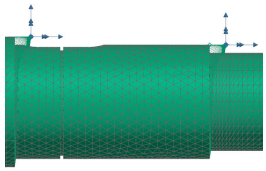
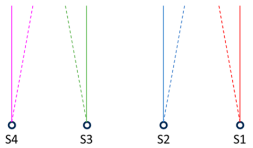
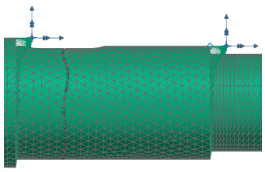
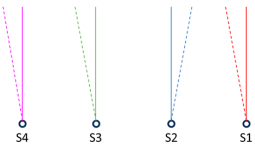
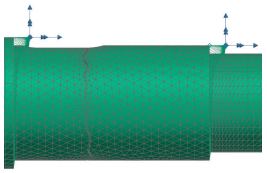
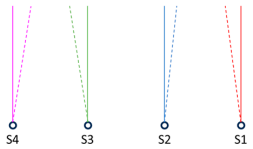
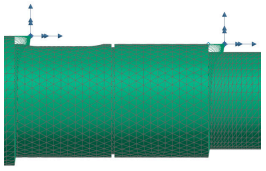
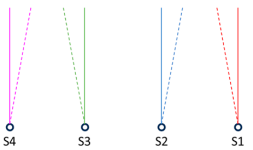
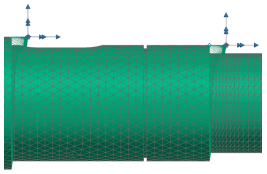
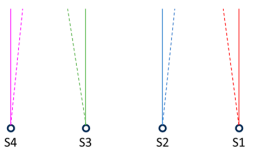
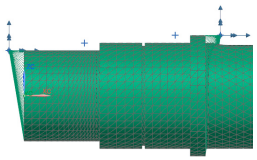
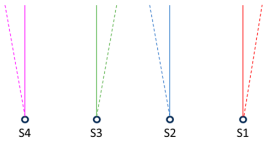
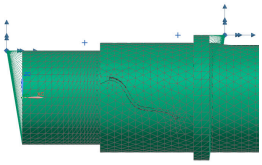
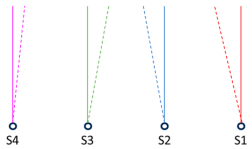
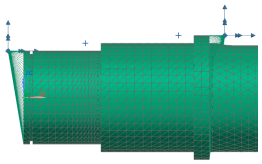
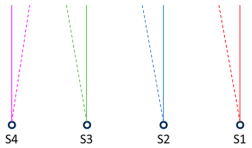
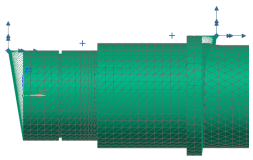
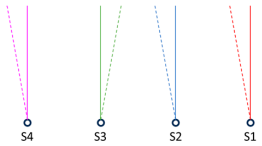
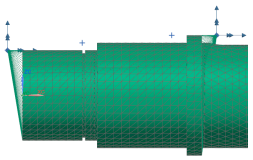
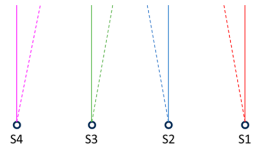
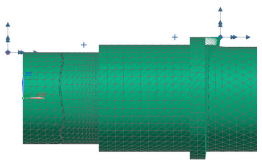
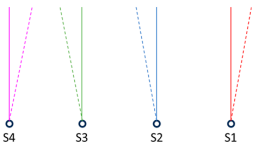
Geometric Form and Place of Damage	Characteristics of Monitored Machine Component State	Deviation of the Characteristics [rad]	Volume Loss [%]	Natural Vibrations Frequency [Hz]
		$\Delta\varphi_1 = 1.17 * 10^7$ $\Delta\varphi_2 = -4.177 * 10^8$ $\Delta\varphi_3 = 1.725 * 10^7$ $\Delta\varphi_4 = -1.716 * 10^8$	0.07	$f_1 = 3.976 * 10^3$ $f_2 = 4.025 * 10^3$ $f_3 = 8.936 * 10^3$ $f_4 = 9.120 * 10^3$
		$\Delta\varphi_1 = 3.074 * 10^6$ $\Delta\varphi_2 = -2.255 * 10^8$ $\Delta\varphi_3 = 8.165 * 10^6$ $\Delta\varphi_4 = -9.489 * 10^6$	0.06	$f_1 = 3.979 * 10^3$ $f_2 = 4.049 * 10^3$ $f_3 = 8.974 * 10^3$ $f_4 = 9.130 * 10^3$
		$\Delta\varphi_1 = 1.368 * 10^7$ $\Delta\varphi_2 = -1.813 * 10^8$ $\Delta\varphi_3 = 5.374 * 10^6$ $\Delta\varphi_4 = 7.069 * 10^7$	0.03	$f_1 = 3.982 * 10^3$ $f_2 = 4.051 * 10^3$ $f_3 = 8.983 * 10^3$ $f_4 = 9.135 * 10^3$
		$\Delta\varphi_1 = 3.808 * 10^7$ $\Delta\varphi_2 = -1.599 * 10^8$ $\Delta\varphi_3 = 6.821 * 10^6$ $\Delta\varphi_4 = -9.874 * 10^7$	0.04	$f_1 = 3.980 * 10^3$ $f_2 = 4.049 * 10^3$ $f_3 = 8.991 * 10^3$ $f_4 = 9.140 * 10^3$
		$\Delta\varphi_1 = 3.161 * 10^7$ $\Delta\varphi_2 = -1.281 * 10^8$ $\Delta\varphi_3 = 7.445 * 10^6$ $\Delta\varphi_4 = -2.198 * 10^8$	0.07	$f_1 = 3.977 * 10^3$ $f_2 = 4.047 * 10^3$ $f_3 = 8.992 * 10^3$ $f_4 = 9.157 * 10^3$
		$\Delta\varphi_1 = 3.917 * 10^7$ $\Delta\varphi_2 = -7.515 * 10^7$ $\Delta\varphi_3 = 5.881 * 10^6$ $\Delta\varphi_4 = -2.469 * 10^8$	0.07	$f_1 = 3.978 * 10^3$ $f_2 = 4.046 * 10^3$ $f_3 = 9.008 * 10^3$ $f_4 = 9.161 * 10^3$

Table 4. Determining the characteristics of the monitored machine component state when introducing damage in the area confined by sensors S3 and S4.

Geometric Form and Place of Damage	Characteristics of Monitored Machine Component State	Deviation of the Characteristics [rad]	Volume Loss [%]	Natural Vibrations Frequency [Hz]
		$\Delta\varphi_1 = -1.748 * 10^7$ $\Delta\varphi_2 = 7.604 * 10^6$ $\Delta\varphi_3 = -8.184 * 10^5$ $\Delta\varphi_4 = 4.792 * 10^7$	0.07	$f_1 = 3.993 * 10^3$ $f_2 = 4.060 * 10^3$ $f_3 = 8.995 * 10^3$ $f_4 = 9.138 * 10^3$
		$\Delta\varphi_1 = 1.684 * 10^6$ $\Delta\varphi_2 = 4.718 * 10^7$ $\Delta\varphi_3 = -1.039 * 10^6$ $\Delta\varphi_4 = -4.664 * 10^7$	0.02	$f_1 = 3.996 * 10^3$ $f_2 = 4.062 * 10^3$ $f_3 = 9.015 * 10^3$ $f_4 = 9.156 * 10^3$
		$\Delta\varphi_1 = 7.296 * 10^7$ $\Delta\varphi_2 = 1.957 * 10^7$ $\Delta\varphi_3 = 4.961 * 10^5$ $\Delta\varphi_4 = -1.231 * 10^8$	0.06	$f_1 = 3.999 * 10^3$ $f_2 = 4.066 * 10^3$ $f_3 = 9.026 * 10^3$ $f_4 = 9.170 * 10^3$
		$\Delta\varphi_1 = 6.842 * 10^6$ $\Delta\varphi_2 = 3.004 * 10^7$ $\Delta\varphi_3 = -1.238 * 10^6$ $\Delta\varphi_4 = 8.088 * 10^6$	0.06	$f_1 = 3.997 * 10^3$ $f_2 = 4.064 * 10^3$ $f_3 = 9.019 * 10^3$ $f_4 = 9.163 * 10^3$
		$\Delta\varphi_1 = 2.779 * 10^7$ $\Delta\varphi_2 = 1.246 * 10^8$ $\Delta\varphi_3 = -2.175 * 10^6$ $\Delta\varphi_4 = -1.757 * 10^8$	0.06	$f_1 = 3.996 * 10^3$ $f_2 = 4.063 * 10^3$ $f_3 = 9.010 * 10^3$ $f_4 = 9.154 * 10^3$
		$\Delta\varphi_1 = -1.657 * 10^7$ $\Delta\varphi_2 = 2.79 * 10^7$ $\Delta\varphi_3 = 4.063 * 10^8$ $\Delta\varphi_4 = -2.881 * 10^{10}$	0.03	$f_1 = 3.991 * 10^3$ $f_2 = 4.063 * 10^3$ $f_3 = 8.986 * 10^3$ $f_4 = 9.153 * 10^3$

Analyzing the test results, it can be noticed that in several cases the form of the state characteristics does not contain deviations consistent with theoretical considerations (Table 4, items 2, 3, 5). It can also be noticed that despite the described condition characteristics (Table 4, item 6), the probable area of damage does not overlap the area where the damage was introduced. However, the following additional criteria can be introduced to identify the damaged area of the monitored machine component:

- In the case of the state characteristics in accordance with Table 4, item 6 and Table 2, item 5, the sum of the absolute values of deviations between sensor monitoring areas where deviations of opposite signs occur should be additionally verified. The damaged area should be considered the area with the highest value of this sum (regardless of the shape of the deviation);

- If the form of the state characteristics does not contain deviations consistent with theoretical considerations (Table 4, items 2, 3, 5), it should be assumed that the damage occurs in the area near the sensor which recorded the largest deviation (in the analyzed cases, it was always the end of the monitored shaft).

Based on the analysis of the results, it can be concluded that the described approach allows one to clearly determine the area of damage (in accordance with the adopted theoretical considerations), when these areas are located between the forces acting on the tested machine component. However, the methodology, improved by additional criteria, enables unambiguous identification of the area of damage in all tested compartments. It should be emphasized, however, that the additional criteria were well adapted to testing four areas with a specific distribution of torques. Therefore, additional tests need to be carried out to confirm their correctness. In further work, the authors will take the following actions to clarify information about the damaged area of the monitored machine component:

- Introducing more sensors for narrowing the areas subject to monitoring and diagnostics;
- Extending the digital model with a model representing transverse vibrations;
- Determining, based on theoretical considerations, the form of the state characteristics in relation to areas lying outside the area of action of forces (torques) on the analyzed machine component.

5. Conclusions

This work concerned the formulation and formalization of a non-invasive method for continuous monitoring of machine components in real time. The formalized mathematical model presented in this work determines proper coupling of the digital model (discrete vibrating model) with the sensors located on the monitored device. Based on the formulated method, damage to the machine component is detected at an early stage of its development, which is often not possible by using classic non-destructive diagnostics methods. In the case of such a monitoring and diagnostic method, a series of verification tests were carried out using an machine component designed in the PLM Siemens NX program in the form of a gear shaft with bearings, which fully recreated the operating conditions of the real machine component. Four acceleration sensors were placed on the machine component in places between which the minor damage was introduced in relation to the volume of the tested system. Due to the number of sensors used (in the context of the number of monitored areas), a discrete vibrating system with four degrees of freedom was built. The discrete system obtained in this way, called in the work a digital monitoring system, was connected to the tested machine component in accordance with a formalized mathematical model.

The application of the DS concept allowed for the acquisition of data obtained from a virtual object and, based on them, the definition of rules allowing for the diagnosis of the machine condition (shaft damage). Moreover, the application of the DS concept for research did not determine the necessity of conducting the inference process in real time. In the case of applying the method presented in this paper to a real object, the DT concept can be applied, where based on real measurements and the developed database of diagnostic rules, it will be possible to automatically infer the condition of the object.

Based on the tests, a regularity can be noticed in the case of damage between the sensors. The observed regularity is the deviation of the time characteristics, processed by the digital shadow in relation to the pattern generated in the initial stage of operation of the monitored system. As a result of damage in the tested machine component, deviation in the response of time processes to the inertial elements of the digital monitoring system (CSM) occurs. The CSM inertial elements on which significant differences in deviations in the state characteristics were observed correspond to the sensors located on the machine component between which the damage was simulated. Three areas were monitored, where in the first two, a deviation of the external state characteristics relative to the reference was observed, which indicated the occurrence of damage in this area. Characteristics of the areas between the forces applied to the machine component (sensors S1, S2, S3) and the type of vibrations considered (angular displacements) are the form of the described

deviation. Based on the test results, it was also observed that for continuous systems, a deviation of the characteristics in all inertial elements of the CSM occurs. In such cases, the deviation values of all characteristics should be compared and the location of the damage should be determined in accordance with the suggested criteria described in Section 4.

To generalize the interpretation of the results, the authors planned the tests taking into account the displacements of the tested machine component in various directions during its movement, which will also enable determining the sensitivity of the formulated method due to the type of vibrations of the considered machine component. In addition, the authors also intend to test the impact of the number of sensors on the form of the state characteristics results. From the results of the tests, it can be concluded that the type of simulated damage had no impact on the determination of the area of its occurrence, and the direction of deviation of the state characteristics was similar in most of the considered cases. Values of the first four natural vibration frequencies of the monitored machine component before and after damage were determined to verify the method. As a result of comparing the determined frequencies, it would be difficult to clearly state that there was damage in the system and to indicate its location in the real machine component. In the future, the authors intend to extend the method by providing qualitative and quantitative data about the damage in a real machine component. It should be mentioned that in addition to the monitoring method formalized in this work, it was also suggested to select the parameters of a discrete system (digital monitoring system) depending on the type of vibrations considered. The parameters of the discrete vibrating system were selected due to the desired dynamic properties in the form of the natural vibration frequency of the monitored machine component and the law of conservation of mass. As a result of the synthesis, a set of six solutions was obtained that met the desired properties of the sought discrete system, of which one was selected which was closest to the RFE (rigid finite element) method. In the future, the authors plan the tests aimed at selecting the optimal tuning of CSM parameters due to the sensitivity of the method for monitoring real machine components formulated in this work. The suggested task of synthesizing the discrete vibrating systems with respect to the desired dynamic properties and mass distribution may contribute to the development of a new approach to creating a discrete model corresponding to real systems and their physical properties.

The application of the developed method to monitoring real machine elements will require the representation of the real load in a digital diagnostic system. Although machines often operate in predictable conditions in terms of the nature and value of the load, an important research issue in this context should be to conduct research to determine the sensitivity of the proposed method to changes in the load value, structure and parameters of the digital diagnostic model. Another problem to be solved in the case of using this method to monitor real machine elements is the selection of appropriate sensors in terms of their operating conditions, installation method and data acquisition.

Author Contributions: Conceptualization: A.D., T.D., K.H. and P.O.; methodology: A.D., T.D., K.H. and K.S.; software: T.D. and K.H.; validation: A.D. and K.B.; formal analysis: Z.M. and C.G.; investigation, K.H.; resources: P.O. and K.B.; data curation: A.D. and T.D.; writing—original draft preparation: A.D. and K.H.; writing—review and editing: K.B. and Z.M.; visualization: K.H. and K.S.; supervision, A.D. and C.G.; project administration: C.G. All authors have read and agreed to the published version of the manuscript.

Funding: This research received no external funding.

Institutional Review Board Statement: Not applicable.

Informed Consent Statement: Not applicable.

Data Availability Statement: The original contributions presented in the study are included in the article, further inquiries can be directed to the corresponding author.

Conflicts of Interest: The authors declare no conflict of interest.

References

1. Aleš, Z.; Pavlů, J.; Legát, V.; Mošna, F.; Jurča, V. Methodology of overall equipment effectiveness calculation in the context of Industry 4.0 environment. *Eksploat. Niezawodn.—Maint. Reliab.* **2019**, *21*, 411–418. [CrossRef]
2. Oztemel, E.; Gursev, S. Literature review of Industry 4.0 and related technologies. *J. Intell. Manuf.* **2020**, *31*, 127–182. [CrossRef]
3. Shyrin, L.; Herasymenko, A.; Inyutkin, I. Modelling the suspended monorail route stresses and deflections during the transport of heavy loads with use of diesel locomotives. *Min. Mach.* **2023**, *41*, 132–142. [CrossRef]
4. Olszyna, G.; Tytko, A. A tool for determining the number of bends and places of accumulation of potential wear of steel ropes operating in the luffing systems of basic opencast mining machines. *Min. Mach.* **2022**, *40*, 229–237. [CrossRef]
5. Gwiazda, A.; Herbuś, K.; Kost, G.; Ociepka, P. Designing mechatronics equipment based on the example of the stewart platform. *Solid State Phenom.* **2015**, *220–221*, 419–422. [CrossRef]
6. Herbuś, K.; Szewerda, K.; Świder, J. Virtual prototyping of the suspended monorail in the aspect of increasing the permissible travel speed in hard coal mines. *Eksploat. Niezawodn.—Maint. Reliab.* **2020**, *22*, 610–619. [CrossRef]
7. Ociepka, P.; Banaś, W.; Herbuś, K.; Kost, G. Simulator of the car for driving courses for the people with mobility impairments. *Adv. Mater. Res.* **2014**, *1036*, 817–822. [CrossRef]
8. Szewerda, K.; Krenicky, T. Use of the MBS method in mining industry R&D projects. *Min. Mach.* **2022**, *40*, 110–120. [CrossRef]
9. Abbate, R.; Caterino, M.; Fera, M.; Caputo, F. Maintenance digital twin using vibration data. *Procedia Comput. Sci.* **2022**, *200*, 546–555. [CrossRef]
10. Bergs, T.; Gierlings, S.; Auerbach, T.; Klink Schraknepper, D.; Augspurger, T. The concept of digital twin and digital shadow in manufacturing. *Procedia CIRP* **2021**, *101*, 81–84. [CrossRef]
11. Jones, D.; Snider, C.; Nassehi, A.; Yon, J.; Hicks, B. Characterizing the digital twin: A systematic literature review. *CIRP J. Manuf. Sci. Technol.* **2020**, *29*, 36–52. [CrossRef]
12. Kritzinger, W.; Karner, M.; Traar, G.; Henjes, J.; Sihn, W. Digital twin in manufacturing: A categorical literature review and classification. In Proceedings of the 16th IFAC Symposium on Information Control Problems in Manufacturing, Bergamo, Italy, 11–13 June 2018; Elsevier: Amsterdam, The Netherlands, 2018; Volume 51, pp. 1016–1022. [CrossRef]
13. Lu, Y.; Liu, C.; Wang, K.I.-K.; Huang, H.; Xu, X. Digital twin-driven smart manufacturing: Connotation, reference model, applications and research issues. *Robot. Comput.-Integr. Manuf.* **2020**, *61*, 101837. [CrossRef]
14. Mi, S.; Feng, Y.; Zheng, H.; Wang, Y.; Gao, Y.; Tan, J. Prediction maintenance integrated decision-making approach supported by digital twin-driven cooperative awareness and interconnection framework. *J. Manuf. Syst.* **2021**, *58*, 329–345. [CrossRef]
15. Qi, Q.; Tao, F. Digital twin and big data towards smart manufacturing and industry 4.0: 360 degree comparison. *IEEE Access* **2018**, *6*, 3585–3593. [CrossRef]
16. VanDerHorn, E.; Wang, Z.; Mahadevan, S. Towards a digital twin approach for vessel-specific fatigue damage monitoring and prognosis. *Reliab. Eng. Syst. Saf.* **2022**, *219*, 108222. [CrossRef]
17. Duan, R.; Lin, Y.; Zeng, Y. Fault diagnosis for complex systems based on reliability analysis and sensors data considering epistemic uncertainty. *Eksploat. Niezawodn.—Maint. Reliab.* **2018**, *20*, 590–601. [CrossRef]
18. Tang, D.; Sheng, W.; Yu, J. Dynamic condition-based maintenance policy for degrading systems described by a random-coefficient autoregressive model: A comparative study. *Eksploat. Niezawodn.—Maint. Reliab.* **2018**, *20*, 590–601. [CrossRef]
19. Zhang, C.; Zhang, Y.; Dui, H.; Wang, S.; Tomovic, M. Importance measure-based maintenance strategy considering maintenance costs. *Eksploat. Niezawodn.—Maint. Reliab.* **2022**, *24*, 15–24. [CrossRef]
20. Kosmol, J. Monitoring, diagnostics and supervision (disscusible paper). *Przetwórstwo Tworzyw* **2015**, *21*, 22–26. (In Polish)
21. Al-Haddad, L.A.; Giernacki, W.; Shandookh, A.A.; Jaber, A.A.; Puchalski, R. Vibration Signal Processing for Multirotor UAVs Fault Diagnosis: Filtering or Multiresolution Analysis? *Eksploat. Niezawodn.—Maint. Reliab.* **2024**, *26*, 176318. [CrossRef]
22. Narendiranath Babu, T.; Manvel Raj, T.; Lakshmanan, T. A Review on Application of Dynamic Parameters of Journal Bearing for Vibration and Condition Monitoring. *J. Mech.* **2015**, *31*, 391–416. [CrossRef]
23. Nowakowski, T.; Komorski, P. Diagnostics of the drive shaft bearing based on vibrations in the high-frequency range as a part of the vehicle's self-diagnostic system. *Eksploat. Niezawodn.—Maint. Reliab.* **2022**, *24*, 70–79. [CrossRef]
24. Puchalski, A.; Komorska, I. Generative modelling of vibration signals in machine maintenance. *Eksploat. Niezawodn.—Maint. Reliab.* **2023**, *25*, 173488. [CrossRef]
25. Umbrajkaar, A.M.; Krishnamoorthy, A.; Dhumale, R.B. Vibration Analysis of Shaft Misalignment Using Machine Learning Approach under Variable Load Conditions. *Shock Vib.* **2020**, *2020*, 1650270. [CrossRef]
26. Wang, T.; Han, Q.; Chu, F.; Feng, Z. Vibration based condition monitoring and fault diagnosis of wind turbine planetary gearbox: A review. *Mech. Syst. Signal Process.* **2019**, *126*, 662–685. [CrossRef]
27. Chung, Y.; Lee, S.; Kim, W. Latest Advances in Common Signal Processing of Pulsed Thermography for Enhanced Detectability: A Review. *Appl. Sci.* **2021**, *11*, 12168. [CrossRef]
28. Chung, Y.; Shrestha, R.; Lee, S.; Kim, W. Thermographic Inspection of Internal Defects in Steel Structures: Analysis of Signal Processing Techniques in Pulsed Thermography. *Sensors* **2020**, *20*, 6015. [CrossRef]
29. Ciampa, F.; Mahmoodi, P.; Pinto, F.; Meo, M. Recent Advances in Active Infrared Thermography for Non-Destructive Testing of Aerospace Components. *Sensors* **2018**, *18*, 609. [CrossRef]
30. Dimitrova, M.; Aminzadeh, A.; Meiabadi, M.S.; Karganroudi, S.S.; Taheri, H.; Ibrahim, H. A Survey on Non-Destructive Smart Inspection of Wind Turbine Blades Based on Industry 4.0 Strategy. *Appl. Mech.* **2022**, *3*, 1299–1326. [CrossRef]

31. Doshvarpassand, S.; Wu, C.; Wang, X. An Overview of Corrosion Defect Characterization Using Active Infrared Thermography. *Infrared Phys. Technol.* **2019**, *96*, 366–389. [CrossRef]
32. Lee, S.; Chung, Y.; Shrestha, R.; Kim, W. Automated Defect Detection Using Threshold Value Classification Based on Thermographic Inspection. *Appl. Sci.* **2021**, *11*, 7870. [CrossRef]
33. Prasad, B.S.; Prabha, K.A.; Kumar, P.V.S.G. Condition Monitoring of Turning Process Using Infrared Thermography Technique—An Experimental Approach. *Infrared Phys. Technol.* **2017**, *81*, 137–147. [CrossRef]
34. Qu, Z.; Jiang, P.; Zhang, W. Development and Application of Infrared Thermography Non-Destructive Testing Techniques. *Sensors* **2020**, *20*, 3851. [CrossRef] [PubMed]
35. Gong, Y.; Guan, L.; Feng, X.; Wang, L.; Yu, X. In-Situ Lubricating Oil Condition Sensoring Method Based on Two-Channel and Differential Dielectric Spectroscopy Combined with Supervised Hierarchical Clustering Analysis. *Chemom. Intell. Lab. Syst.* **2016**, *158*, 155–164. [CrossRef]
36. Shinde, H.M.; Bewoor, A.K. Evaluating Petrol Engine Oil Deterioration through Oxidation and Nitration Parameters by Low-Cost IR Sensor. *Appl. Petrochem. Res.* **2020**, *10*, 83–94. [CrossRef]
37. Wakiru, J.M.; Pintelon, L.; Muchiri, P.N.; Chemweno, P.K. A Review on Lubricant Condition Monitoring Information Analysis for Maintenance Decision Support. Mech. *Syst. Signal Process.* **2019**, *118*, 108–132. [CrossRef]
38. Wolak, A.; Zając, G. The Kinetics of Changes in Kinematic Viscosity of Engine Oils under Similar Operating Conditions. *Eksploat. Niezawodn.—Maint. Reliab.* **2017**, *19*, 260–272. [CrossRef]
39. Zhe, J.; Zhu, X.; Zhong, C. A High Sensitivity Wear Debris Sensor Using Ferrite Cores for Online Oil Condition Monitoring. *Meas. Sci. Technol.* **2017**, *28*, 75–102. [CrossRef]
40. Zhu, X.; Zhong, C.; Zhe, J. Lubricating Oil Conditioning Sensors for Online Machine Health Monitoring—A Review. *Tribol. Int.* **2017**, *109*, 473–484. [CrossRef]
41. Caggiano, A.; Zhang, J.; Alfieri, V.; Caiazzo, F.; Gao, R.; Teti, R. Machine learning-based image processing for on-line defect recognition in additive manufacturing. *CIRP Ann.* **2019**, *68*, 451–454. [CrossRef]
42. Dutta, S.; Pal, S.K.; Sen, R. On-machine tool prediction of flank wear from machined surface images using texture analyses and support vector regression. *Precis. Eng.* **2016**, *43*, 34–42. [CrossRef]
43. Kwon, Y.; Fischer, G.W. A novel approach to quantifying tool wear and tool life measurements for optimal tool management. *Int. J. Mach. Tools Manuf.* **2003**, *43*, 359–368. [CrossRef]
44. Amarnath, M.; Sugumaran, V.; Kumar, H. Exploiting Sound Signals for Fault Diagnosis of Bearings Using Decision Tree. *Measurement* **2013**, *46*, 1250–1256. [CrossRef]
45. Ghaderi, H.; Kabiri, P. Automobile Engine Condition Monitoring Using Sound Emission. *Turk. J. Electr. Eng. Comput. Sci.* **2017**, *25*, 1807–1826. [CrossRef]
46. Li, Z.; Lv, Y.; Yuan, R.; Zhang, Q. Multi-Fault Diagnosis of Rotating Machinery via Iterative Multivariate Variational Mode Decomposition. *Meas. Sci. Technol.* **2022**, *33*, 125104. [CrossRef]
47. Sharan, R.; Xiong, H.; Berkovsky, S. Benchmarking Audio Signal Representation Techniques for Classification with Convolutional Neural Networks. *Sensors* **2021**, *21*, 3434. [CrossRef]
48. Shiri, H.; Wodecki, J.; Ziętek, B.; Zimroz, R. Inspection Robotic UGV Platform and the Proce-dure for an Acoustic Signal-Based Fault Detection in Belt Conveyor Idler. *Energies* **2021**, *14*, 7646. [CrossRef]
49. Asad, B.; Vaimann, T.; Rassõlkin, A.; Kallaste, A.; Belahcen, A. Review of Electrical Machine Diagnostic Methods Applicability in the Perspective of Industry 4.0. *Electr. Control Commun. Eng.* **2018**, *14*, 108–116. [CrossRef]
50. Chaulya, S.K.; Prasad, G.M. Formation of digital mine using the internet of things. In *Sensing and Monitoring Technologies for Mines and Hazardous Areas*; Elsevier: Amsterdam, The Netherlands, 2016; pp. 279–350. [CrossRef]
51. Garcia-Calva, T.A.; Morinigo-Sotelo, D.; de Jesus Romero-Troncoso, R. Non-Uniform Time Resampling for Diagnosing Broken Rotor Bars in Inverter-Fed Induction Motors. *IEEE Trans. Ind. Electron.* **2017**, *64*, 2306–2315. [CrossRef]
52. Li, M.; Lu, Q.; Bai, S.; Zhang, M.; Tian, H.; Qin, L. Digital twin-driven virtual sensor approach for safe construction operations of trailing suction hopper dredger. *Autom. Constr.* **2021**, *132*, 103961. [CrossRef]
53. Liu, M.; Fang, S.; Dong, H.; Xu, C. Review of digital twin about concepts, technologies, and industrial applications. *J. Manuf. Syst.* **2021**, *58*, 346–361. [CrossRef]
54. Sapena-Bano, A.; Pineda-Sanchez, M.; Puche-Panadero, R.; Martinez-Roman, J.; Matic, D. Fault Diagnosis of Rotating Electrical Machines in Transient Regime Using a Single Stator Current's FFT. *IEEE Trans. Instrum. Meas.* **2015**, *64*, 3137–3146. [CrossRef]
55. Silvestri, L.; Forcina, A.; Introna, V.; Santolamazza, A.; Cesarotti, V. Maintenance transformation through Industry 4.0 technologies: A systematic literature review. *Comput. Ind.* **2020**, *123*, 103335. [CrossRef]
56. Wang, K.-J.; Lee, Y.-H.; Angelica, S. Digital twin design for real-time monitoring—A case study of die cutting machine. *Int. J. Prod. Res.* **2021**, *59*, 6471–6485. [CrossRef]
57. Xiong, M.; Wang, H.; Fu, Q.; Xu, Y. Digital twin–driven aero-engine intelligent predictive maintenance. *Int. J. Adv. Manuf. Technol.* **2021**, *114*, 3751–3761. [CrossRef]
58. Xu, B.; Sun, L.; Xu, L.; Xu, G. Improvement of the Hilbert Method via ESPRIT for Detecting Rotor Fault in Induction Motors at Low Slip. *IEEE Trans. Energy Convers.* **2013**, *28*, 225–233. [CrossRef]

59. Yahia, K.; Cardoso, A.J.M.; Ghoggal, A.; Zouzou, S.-E. Induction Motors Broken Rotor Bars Diagnosis Through the Discrete Wavelet Transform of the Instantaneous Reactive Power Signal under Time-varying Load Conditions. *Electr. Power Compon. Syst.* **2014**, *42*, 682–692. [CrossRef]
60. You, Y.; Chen, C.; Hu, F.; Liu, Y.; Ji, Z. Advances of digital twins for predictive maintenance. *Procedia Comput. Sci.* **2022**, *200*, 1471–1480. [CrossRef]
61. Yu, J.; Liu, P.; Li, Z. Hybrid modelling and digital twin development of a steam turbine control stage for online performance monitoring. *Renew. Sustain. Energy Rev.* **2020**, *133*, 110077. [CrossRef]
62. Zonta, T.; da Costa, C.A.; Righi, R.d.R.; de Lima, M.J.; da Trindade, E.S.; Li, G.P. Predictive maintenance in the industry 4.0: A systematic literature review. *Comput. Ind. Eng.* **2020**, *150*, 106889. [CrossRef]
63. Malla, C.; Panigrahi, I. Review of Condition Monitoring of Rolling Element Bearing Using Vibration Analysis and Other Techniques. *J. Vib. Eng. Technol.* **2019**, *7*, 407–414. [CrossRef]
64. Souflas, I.; Pezouvanis, A.; Ebrahimi, K. Health monitoring system for transmission shafts based on adaptive parameter identification. *Mech. Syst. Signal Process.* **2018**, *104*, 673–687. [CrossRef]
65. Chin, C.; Abdullah, S.; Ariffin, A.; Singh, S.; Arifin, A. A review of the wavelet transform for durability and structural health monitoring in automotive applications. *Alex. Eng. J.* **2024**, *99*, 204–216. [CrossRef]
66. Rehman, S.U.; Usman, M.; Toor, M.H.Y.; Hussaini, Q.A. Advancing structural health monitoring: A vibration-based IoT approach for remote real-time systems. *Sens. Actuators A Phys.* **2024**, *365*, 114863. [CrossRef]
67. Mei, S.; Yuan, M.; Cui, J.; Dong, S.; Zhao, J. Machinery condition monitoring in the era of industry 4.0: A relative degree of contribution feature selection and deep residual network combined approach. *Comput. Ind. Eng.* **2022**, *168*, 108129. [CrossRef]
68. Zhang, G.; Wang, Y.; Li, X.; Qin, Y.; Tang, B. Health indicator based on signal probability distribution measures for machinery condition monitoring. *Mech. Syst. Signal Process.* **2023**, *198*, 110460. [CrossRef]
69. Xie, J.; Liu, J.; Chen, J.; Zi, Y. Blade damage monitoring method base on frequency domain statistical index of shaft's random vibration. *Mech. Syst. Signal Process.* **2022**, *165*, 108351. [CrossRef]
70. Xiao, Y.; Wang, S.; Dong, J.; Wang, S.; Xia, C. Online monitoring method of non-cylindrical wheel wear for gear grinding based on dynamic force model. *Mech. Syst. Signal Process.* **2024**, *206*, 110915. [CrossRef]
71. Thibault, N.; Bourdon, A.; Rémond, D.; Lecouvreur, D. Dynamic models for power transmission monitoring in non-stationary conditions based on IAS signals. *Mech. Mach. Theory* **2024**, *201*, 105733. [CrossRef]
72. Karyofyllas, G.; Giagopoulos, D. Condition monitoring framework for damage identification in CFRP rotating shafts using Model-Driven Machine learning techniques. *Eng. Fail. Anal.* **2024**, *158*, 108052. [CrossRef]
73. Deraemaeker, A.; Preumont, A. Vibration based damage detection using large array sensors and spatial filters. *Mech. Syst. Signal Process.* **2006**, *20*, 1615–1630. [CrossRef]
74. Bahlous, S.E.O.; Abdelghani, M.; Smaoui, H.; El-Borgi, S. A Modal Filtering and Statistical Approach for Damage Detection and Diagnosis in Structures using Ambient Vibrations Measurements. *J. Vib. Control* **2007**, *13*, 281–308. [CrossRef]
75. Mendrok, K.; Uhl, T. Overview of modal model based damage detection methods. In Proceedings of the 2004 ISMA, Leuven, Belgium, 20–22 September 2004.
76. Sohn, H.; Law, K.H. Extraction of Ritz Vectors from Vibration Test Data. *Mech. Syst. Signal Process.* **2001**, *15*, 213–226. [CrossRef]
77. Mendrok, K. Comparison of Damage Detection Methods in Aspect of Their Automation Ability. *DIAGNOSTYKA* **2007**. Available online: http://www.diagnostyka.net.pl/DIAGNOSTYKA-3-43-2007,81338,0,2.html (accessed on 25 October 2024). (In Polish)
78. Mohamed, A.; Neilson, R.; MacConnell, P.; Renton, N.; Deans, W. Monitoring of Fatigue Crack Stages in a High Carbon Steel Rotating Shaft Using Vibration. *Procedia Eng.* **2011**, *10*, 130–135. [CrossRef]
79. Valdez-Yepez, R.; Tutivén, C.; Vidal, Y. Structural health monitoring of jacket-type support structures in offshore wind turbines: A comprehensive dataset for bolt loosening detection through vibrational analysis. *Data Brief* **2024**, *53*, 110222. [CrossRef]
80. Chen, B.; Zang, C. Artificial immune pattern recognition for structure damage classification. *Comput. Struct.* **2009**, *87*, 1394–1407. [CrossRef]
81. Anaya, M.; Tibaduiza, D.; Pozo, F. Data driven methodology based on artificial immune systems for damage detection. In Proceedings of the 7th European Workshop on Structural Health Monitoring, Nantes, France, 8–11 July 2014.
82. Dasgupta, D.; KrishnaKumar, K.; Wong, D.; Berry, M. Negative Selection Algorithm for Aircraft Fault Detection. Artificial Immune Systems. In *Artificial Immune Systems, Proceedings of the ICARIS 2004, Catania, Italy, 13–16 September 2004*; Lecture Notes in Computer Science; Springer: Berlin/Heidelberg, Germany, 2004; Volume 3239, p. 3239. [CrossRef]
83. Meyes, R.; Donauer, J.; Schmeing, A.; Meisen, T. A Recurrent Neural Network Architecture for Failure Prediction in Deep Drawing Sensory Time Series Data. *Procedia Manuf.* **2019**, *34*, 789–797. [CrossRef]
84. Kutyłowska, M. Neural network approach for failure rate prediction. *Eng. Fail. Anal.* **2015**, *47*, 41–48. [CrossRef]
85. Khakzad, N.; Khan, F.; Amyotte, P.; Cozzani, V. Domino effect analysis using Bayesian networks. *Risk Anal.* **2013**, *33*, 292–306. [CrossRef]
86. Guo, L.; Wang, Z. Analysis of uncertainty propagation path of fire-induced domino effect based on an approach of layered fuzzy Petri nets. *Chem. Eng. Sci.* **2023**, *268*, 118410. [CrossRef]
87. Yan, A.; Wang, W.; Zhang, C.; Zhao, H. A fault prediction method that uses improved case-based reasoning to continuously predict the status of a shaft furnace. *Inf. Sci.* **2014**, *259*, 269–281. [CrossRef]

88. Dou, D.; Yang, J.; Liu, J.; Zhao, Y. A rule-based intelligent method for fault diagnosis of rotating machinery. *Knowl.-Based Syst.* **2012**, *36*, 1–8. [CrossRef]
89. Bruyneel, M.; Naito, T.; Urushiyama, Y.; McDougall, S. Predictive Simulations of Damage Propagation in Laminated Composite Materials and Structures with LMS Samtech Samcef. In Proceedings of the SAE 2015 World Congress, Detroit, MI, USA, 21–23 April 2015; Conference Paper in SAE Technical Papers. [CrossRef]
90. Frick, N.; Terwolbeck, J.; Seibel, B.; Metternich, J. Design Model for the Digital Shadow of a Value Stream. *Systems* **2024**, *12*, 20. [CrossRef]
91. Liebenberg, M.; Jarke, M. Information Systems Engineering with Digital Shadows: Concept and Case Studies. In *Advanced Information Systems Engineering, Proceedings of the 32nd International Conference, CAiSE 2020, Grenoble, France, 8–12 June 2020*; Springer: Cham, Switzerland, 2020; pp. 70–84. [CrossRef]
92. Liebenberg, M.; Jarke, M. Information systems engineering with Digital Shadows: Concept and use cases in the Internet of Production. *Inf. Syst.* **2023**, *114*, 102182. [CrossRef]
93. Dymarek, A.; Dzitkowski, T.; Banaś, W. *Sposób oceny stopnia zużycia obiektów narażonych na działanie obciążeń dynamicznych*; Politechnika Śląska: Gliwice, Poland, 2023; p. 446566.
94. Dymarek, A.; Dzitkowski, T. The use of synthesis methods in position optimisation and selection of tuned mass damper (TMD) parameters for systems with many degrees of freedom. *Arch. Control Sci.* **2021**, *31*, 185–211. [CrossRef]
95. Dzitkowski, T.; Dymarek, A.; Margielewicz, J.; Gąska, D.; Orzech, L.; Lesiak, K. Designing of drive systems in the aspect of the desired spectrum of operation. *Energies* **2021**, *14*, 2562. [CrossRef]
96. Białas, K.; Dymarek, A.; Dzitkowski, T. Impact of 3D printer vibration reduction on the quality of its printout. *Int. J. Mod. Manuf. Technol.* **2023**, *15*, 79–90. [CrossRef]

Disclaimer/Publisher's Note: The statements, opinions and data contained in all publications are solely those of the individual author(s) and contributor(s) and not of MDPI and/or the editor(s). MDPI and/or the editor(s) disclaim responsibility for any injury to people or property resulting from any ideas, methods, instructions or products referred to in the content.